JOURNAL OF PROPULSION AND POWER
Vol. 16, No. 6, November–December 2000

Linear Versus Quadratic Amplitude Feedback in Active Control of Compressor Rotating Stall

Nikos Markopoulos,* Yedidia Neumeier,† J. V. R. Prasad,‡ and Ben T. Zinn§
Georgia Institute of Technology, Atlanta, Georgia 30332-0150

Several issues that have been overlooked or only partially addressed in previous literature related to the active control of compressor rotating stall are clarified. This is accomplished via a detailed local stability analysis of the rotating stall inception point and the locally branched unstalled and stalled equilibria. The analysis is based on the first-term Galerkin approximation of the Moore–Greitzer model (Moore, F. K., and Greitzer, E. M., "A Theory of Post-Stall Transients in Axial Compressor Systems, Part 1, Development of Equations," ***Journal of Turbomachinery*****, 1986), and it is valid for an arbitrary compressor map and a parabolic throttle characteristic. It is generically performed for a rather large class of throttle feedback control laws. Each such law is proportional to the rotating stall amplitude, raised to a strictly positive exponent. The proportionality constant is a nonnegative feedback gain. It is shown that linear feedback renders the rotating stall inception point and the neighboring stalled branch locally asymptotically stable for any value of the feedback gain. Quadratic feedback on the other hand represents a limiting case of control effectiveness and can at best lead to conditional local stability; that is, it can render the stall inception point and the neighboring stalled branch locally asymptotically stable only for sufficiently high values of the feedback gain. Finally, sublinear feedback, namely, feedback with an exponent less than unity, not only unconditionally stabilizes the stall inception point and the neighboring stalled branch, but also completely smooths out any transition to rotating stall. These results extend and in some places contrast previous work on the subject that has dismissed such linear or sublinear feedback and concentrated mainly on quadratic feedback as a viable means of controlling compressor rotating stall.**

Nomenclature

A	=	rotating stall amplitude
a_i, b_i, c_i	=	auxiliary constants, defined (for $i = 1, 2, 3$) in Eqs. (21–23)
C_i, D_i	=	auxiliary constants, defined (for $i = 1, 2$) in Eqs. (57) and (58)
E	=	auxiliary variable, equal to A^p
$F(\Phi, A)$	=	first Moore–Greitzer integral, Eq. (6)
$G(\Phi, A)$	=	second Moore–Greitzer integral, Eq. (7)
h, w	=	functions representing the center manifold, Eqs. (43), (44), (46), and (47)
J	=	Jacobian matrix or its particular element (as denoted by subscript), Eqs. (38), (64), and (74)
k	=	feedback gain, Eq. (10)
k_{crit}	=	critical value of k, Eqs. (33) and (34)
L	=	Lyapunov function, Eq. (56)
M	=	positive constant from Moore–Greitzer theory[3]
m	=	constant representing the mass of the air enclosed in the compressor cavity
N_e	=	auxiliary constant, Eq. (76)
p	=	strictly positive feedback exponent, Eq. (10)
$Q(\Phi, A)$	=	generating function for $F(\Phi, A)$ and $G(\Phi, A)$, Appendix B, Eq. (B1)
S	=	generalized throttle valve area (control)
t	=	time
u_d	=	infinitesimal throttle valve area disturbance
V	=	constant characterizing the plenum volume
x_1	=	perturbation in Φ, measured from the stall inception point, Eq. (16)
x_2	=	perturbation in ΔP, measured from the stall inception point, Eq. (16)
x_3	=	perturbation in A, measured from the stall inception point, Eq. (16)
y_3	=	transformed state, see Eq. (24)
$\alpha_i, \beta, \gamma_i$	=	auxiliary constants ($i = 1, 2$) defined in Eqs. (54) and (55)
ΔP	=	pressure rise across the compressor cavity
$\delta^j f_{j\kappa}$	=	functions representing higher-order terms, Eqs. (18–20) and (25–27)
$\delta^j g_{j\kappa}$	=	functions representing higher-order terms, Eqs. (51–53)
η, μ, ν	=	coefficients of characteristic equation, Eqs. (39) and (66)
θ	=	azimuth angle
λ	=	characteristic equation variable, Eqs. (39), (65), and (66)
ξ_i	=	nondimensional variables corresponding to x_i (for $i = 1, 2, 3$), Eqs. (49) and (50)
τ	=	nondimensional time, Eq. (49)
Φ	=	circumferentially averaged axial flow speed through the compressor cavity, Eq. (5)
ϕ	=	axial velocity component of flow through the compressor cavity
Ψ	=	compressor blade aerodynamic force characteristic

Subscripts

e	=	equilibrium state other than the stall inception point
Ψ', etc.	=	derivatives of $\Psi(\phi)$ with respect to ϕ
0	=	equilibrium state at the stall inception point

Received 4 March 1999; revision received 29 November 1999; accepted for publication 2 December 1999.

*Postdoctoral Fellow, School of Aerospace Engineering. Member AIAA.
†Senior Research Engineer, School of Aerospace Engineering. Member AIAA.
‡Associate Professor, School of Aerospace Engineering. Senior Member AIAA.
§David S. Lewis Jr. Chair and Regents' Professor, School of Aerospace Engineering. Fellow AIAA.

I. Introduction

COMPRESSORS are routinely used in processes involving pressurized fluids. In axial compressors the kinetic energy of

a set of rotating airfoils is imparted to the fluid moving parallel to the rotation axis. Certain aerodynamic instabilities in compression systems manifest themselves as the phenomenon of compressor rotating stall (RS). This is a two-dimensional flow oscillation that involves a circumferentially rotating partial flow blockage. It results in a loss of compression system performance and operating efficiency. The conventional approach of addressing RS is to constrain compressor operation to a stable region at a safe margin from the stall inception point (SIP). This represents a loss of opportunity of compressor performance. Recent approaches are aimed at reducing or eliminating this stall margin through the use of active control.

Most recent active control strategies[1,2] are based on low-order approximations of the Moore–Greitzer model[3,4] (MG). This consists of a set of nonlinear partial differential equations with periodic boundary conditions. Using a first-term Galerkin approximation of MG, previous studies[5,6] have established a qualitative match between dynamic structure and experimental results. Nonlinear control schemes with control proportional to the square of the RS amplitude have been proposed and analyzed, theoretically,[7] numerically[8] and experimentally[9] by combining nonlinear dynamics and bifurcation theory.[10,11] In Ref. 7, a control law with linear terms, in addition to quadratic and cubic terms, has been initially assumed in the general development; the coefficients of the linear terms have been taken as zero to facilitate the subsequent stability analysis. In particular, to our knowledge, a detailed investigation of the effect of more general control laws on the local stability of the SIP so far has not been carried out in a systematic way. This study is aimed at filling this void by considering a general representation of RS feedback control to be proportional to a nonnegative power of RS amplitude. Section VII supplies a quick review of all of the results shown in this paper.

II. Compressor Model

The model that we examine, giving rise to the RS instability, is the first-term Galerkin approximation of the MG.[3] We will refer to it simply as the MG. It is described by

$$\frac{d\Phi}{dt} = \frac{1}{2\pi m}\int_0^{2\pi} \Psi(\Phi + A\sin\theta)\,d\theta - \frac{\Delta P}{m} \tag{1}$$

$$\frac{d(\Delta P)}{dt} = \frac{1}{V}\left(\Phi - S\sqrt{\Delta P}\right) \tag{2}$$

$$\frac{dA}{dt} = \frac{M}{2\pi}\int_0^{2\pi} \Psi(\Phi + A\sin\theta)\sin\theta\,d\theta \tag{3}$$

These equations are based on several assumptions and approximations. At the compressor cavity (see Fig. 1) the Mach number is assumed to be low, and so the airflow is modeled as incompressible.[3] Compressibility effects are taken into account at the plenum.[3] At the cavity the flow is further assumed to be purely axial, but not necessarily uniform.[3] It is described by an axial velocity component $\phi(\theta, t)$ that varies along the circumference. The first harmonic of $\phi(\theta, t)$ with respect to a properly chosen reference frame[3] is given by

$$\phi(\theta, t) = \Phi(t) + A(t)\sin\theta \tag{4}$$

where Φ is the average value of ϕ along the circumference,

$$\Phi(t) = \frac{1}{2\pi}\int_0^{2\pi} \phi(\theta, t)\,d\theta \tag{5}$$

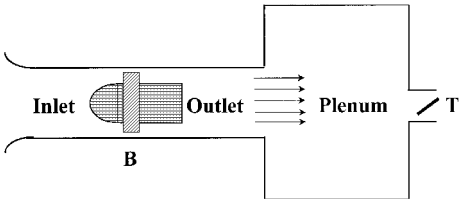

Fig. 1 Schematic model of a compressor.

and A is the amplitude of the velocity perturbation due to the RS. From Eq. (3), zero A at any time implies zero A at all times. Therefore, as A evolves in time, it can never change sign. It can then always be taken as nonnegative. The aerodynamic force per unit cross-sectional area of the cavity, developed by the blades, is[3]

$$F(\Phi, A) = \frac{1}{2\pi}\int_0^{2\pi} \Psi(\Phi + A\sin\theta)\,d\theta \tag{6}$$

where $\Psi(\phi)$ is the compressor blade aerodynamic force characteristic. The acceleration the air experiences in the cavity is equal to the difference between the force per unit cross-sectional area $F(\Phi, A)$ and the pressure rise ΔP across the cavity, divided by a characteristic positive constant m representing the mass of the air enclosed in the cavity. This leads to Eq. (1). The rate of change of ΔP is fixed by the balance between the flow incoming to the plenum from the cavity and the flow outgoing from the plenum through the throttle. A parabolic throttle characteristic then implies Eq. (2). V is a positive constant characterizing the plenum volume, and S represents a generalized throttle valve area. Finally, Eq. (3), characterized by the integral

$$G(\Phi, A) = \frac{1}{2\pi}\int_0^{2\pi} \Psi(\Phi + A\sin\theta)\sin\theta\,d\theta \tag{7}$$

is just a prediction of the MG[3] concerning the dynamics of the RS amplitude. M in Eq. (3) denotes a positive constant that depends on compressor system parameters such as geometry, etc.

III. Operation at or near the SIP

From now on, S will play the role of a control variable. Figure 2 shows qualitatively, in the plane of ΔP, Φ, the locus of equilibria for a typical compressor model, for constant S. Setting the right-hand sides of Eqs. (1) and (3) to zero results in the branches abdsghr and bcfdlkes. The first is the unstalled branch of equilibria (USB). On it, A is zero. The second is the stalled branch of equilibria (SB). On it, A is nonzero. Setting the right-hand side of Eq. (2) to zero, with constant S, results in a parabolic throttle characteristic. Several such characteristics, corresponding to different values of S, are shown in Fig. 2. The intersection of a throttle characteristic and the SB or USB defines a possible operation point. For constant S, bold dashed lines show unstable operation points, whereas bold solid lines show stable operation points. As S is decreased, the throttle characteristic shifts from ohm to oegn to oksp, and the stable operation point shifts from curve h to curve g to curve s. Point s is the SIP. Under operation with no disturbances at SIP, A is identically zero, whereas ΔP is a maximum. If S is decreased beyond its SIP value the stable operation point jumps to the SB, to the left of point k. Thus, during operation under constant S at SIP, an arbitrarily small disturbance in S is enough to throw the compressor into the RS

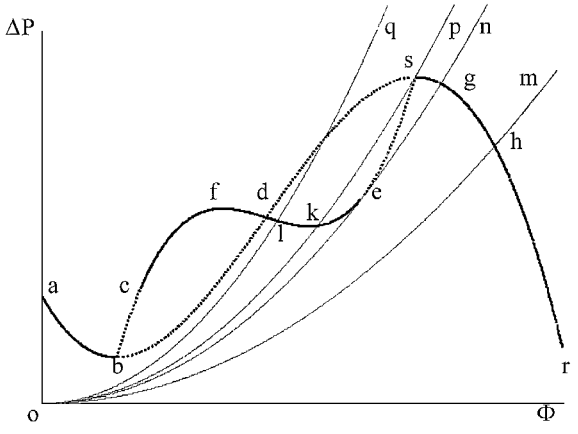

Fig. 2 Qualitative locus of equilibrium points in the ΔP vs Φ plane for a typical compressor under no control, together with four throttle characteristics.

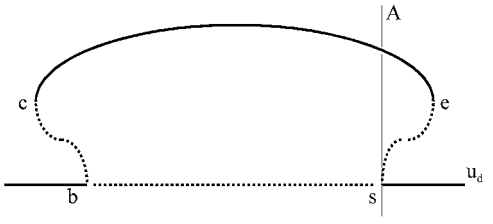

Fig. 3 Qualitative bifurcation diagram for the equilibrium values of A vs u_d under no feedback control ($k = 0$).

regime (point k). Decreasing S further moves the stable operation point toward l. Increasing S moves the stable operation point toward point e and then point g, giving rise to the hysteresis loop skegs. The aim is to vary S to stabilize the compressor at an equilibrium point of Eqs. (1–3) that lies on the USB at or near the SIP. Note that varying S does not affect the SB or USB in Fig. 2. It only affects the stability of points on these branches (redistributing the solid and dashed lines). The SIP will be denoted by the subscript 0. It is characterized by

$$\Psi'(\Phi_0) = 0, \qquad \Psi''(\Phi_0) < 0 \tag{8}$$

For a steady equilibrium at SIP the right-hand sides of Eqs. (1–3) must identically equal zero,

$$A_0 = 0, \qquad \Delta P_0 = \Psi(\Phi_0), \qquad \Phi_0 = S_0\sqrt{\Delta P_0} \tag{9}$$

The equilibrium states Φ_0, ΔP_0, and A_0 and the required control S_0 at SIP are fixed from Eqs. (8) and (9). To stabilize the compressor at or near the SIP, we will assume that the control S is always given by the sum

$$S = S_0 + u_d + kA^p, \qquad k \geq 0, \quad p > 0 \tag{10}$$

where S_0 is the value of S required for operation at SIP, whereas kA^p is a feedback term that we use to render such an operation stable. The term u_d represents a persistent, small, and constant throttle disturbance, over which we have no control. Zero u_d implies an equilibrium at SIP. Small u_d implies an equilibrium near the SIP. Figure 3 shows the locus of equilibrium values A_e of A as a function of u_d for a typical compressor model and under no feedback ($k = 0$). Solid bold and dashed lines indicate stable and unstable equilibria, respectively. Point s, corresponding to $u_d = 0$, denotes the SIP. The RS instability arises because of the jump in the stable equilibrium of A from 0 to a finite value as u_d crosses 0. The axis $A = 0$ represents the axisymmetric branch of equilibria (AB), characterized by an absence of RS and axially symmetric flow through the compressor [$A_e = 0$ and $\phi = \Phi_e$ in Eq. (4)]. The branch secb represents the nonaxisymmetric branch of equilibria (NAB) for which RS is present. From now on the AB or NAB will always refer to the plane of A vs u_d, whereas the SB or USB will always refer to the plane of ΔP vs Φ. We may use these terms interchangeably when no danger of confusion is present. We will present a complete, local stability analysis of the SIP and the neighboring equilibria on the USB and SB for the full system of Eqs. (1–3), under a control S given by Eq. (10), with infinitesimally small u_d.

IV. Integral-Free Form for the MG Model[3]

We start by eliminating the variable θ and expressing the integrals in Eqs. (6) and (7) as an infinite series. This greatly facilitates all of the subsequent analysis. Practically, it can be accomplished most efficiently using the contour integration method of complex analysis.[12] Thus, it is shown in Appendix A that, based on some mild smoothness assumptions on the function Ψ, the two Moore–Greitzer[3] integrals [Eqs. (6) and (7)], are equal to

$$F(\Phi, A) = \sum_{\kappa=0}^{\infty} \frac{\Psi^{2\kappa}(\Phi)}{(\kappa!)^2}\left(\frac{A}{2}\right)^{2\kappa} \tag{11}$$

$$G(\Phi, A) = \sum_{\kappa=1}^{\infty} \frac{\kappa\Psi^{2\kappa-1}(\Phi)}{(\kappa!)^2}\left(\frac{A}{2}\right)^{2\kappa-1} \tag{12}$$

Using these expressions and the control S of Eq. (10), the system of Eqs. (1–3) can be rewritten as

$$\frac{d\Phi}{dt} = -\frac{\Delta P}{m} + \frac{1}{m}\sum_{\kappa=0}^{\infty} \frac{\Psi^{2\kappa}(\Phi)}{(\kappa!)^2}\left(\frac{A}{2}\right)^{2\kappa} \tag{13}$$

$$\frac{d(\Delta P)}{dt} = \frac{1}{V}\left[\Phi - \left(S_0 + u_d + kA^p\right)\sqrt{\Delta P}\,\right] \tag{14}$$

$$\frac{dA}{dt} = M\sum_{\kappa=1}^{\infty} \frac{\kappa\Psi^{2\kappa-1}(\Phi)}{(\kappa!)^2}\left(\frac{A}{2}\right)^{2\kappa-1} \tag{15}$$

Equations (13–15) are completely equivalent to Eqs. (1–3) and (10). Previous studies have implicitly imposed smoothness properties on $\Psi(\phi)$ by working with specific functional forms. By far the most common of these has been a cubic polynomial. Thus, Eqs. (11) and (12) represent a direct generalization on all such results. The behavior of the MG about the SIP becomes very transparent under Eqs. (13–15).

V. Behavior About the SIP

Let x_1, x_2, and x_3 be perturbations in the states of the system of Eqs. (13–15), measured from their corresponding equilibrium values at the SIP [see Eqs. (8) and (9)]. Explicitly,

$$\Phi = \Phi_0 + x_1, \qquad \Delta P = \Delta P_0 + x_2, \qquad A = x_3 \tag{16}$$

The control S [see Eq. (10)] can then be written as

$$S = S_0 + u_d + kx_3^p, \qquad k \geq 0, \quad p > 0 \tag{17}$$

Using these perturbations, rather than the original states, and taking the equilibrium conditions [Eqs. (8) and (9)] into account, it can be shown that the system of Eqs. (13–15) can be written equivalently as

$$\frac{dx_1}{dt} = -a_1x_2 - a_2x_1^2 - a_3x_3^2 + \delta^3 f_1(x_1, x_3) \tag{18}$$

$$\frac{dx_2}{dt} = b_1x_1 - b_2x_2 - \left(u_d + kx_3^p\right)\left[b_3 - \delta^1 f_{21}(x_2)\right] + \delta^2 f_{22}(x_2) \tag{19}$$

$$\frac{dx_3}{dt} = x_3\left[-c_1x_1 + c_2x_3^2 + c_3x_1^2 + \delta^3 f_3(x_1, x_3)\right] \tag{20}$$

where a_i, b_i, and c_i are constants defined as

$$a_1 = \frac{1}{m}, \qquad a_2 = \frac{|\Psi''(\Phi_0)|}{2m}, \qquad a_3 = \frac{|\Psi''(\Phi_0)|}{4m} \tag{21}$$

$$b_1 = \frac{1}{V}, \qquad b_2 = \frac{S_0^2}{2V\Phi_0}, \qquad b_3 = \frac{\Phi_0}{VS_0} \tag{22}$$

$$c_1 = \frac{M|\Psi''(\Phi_0)|}{2}, \qquad c_2 = \frac{M\Psi'''(\Phi_0)}{16}, \qquad c_3 = 4c_2 \tag{23}$$

The functions $\delta^3 f_1$ and $\delta^3 f_3$ in Eqs. (18) and (20) represent an infinite summation of terms in x_1 and x_3 that are of order three or higher. Similarly, the functions $\delta^1 f_{21}$ and $\delta^2 f_{22}$ in Eq. (19) represent an infinite summation of terms in x_2 that are of order one and two or higher, respectively. For the local stability analysis of Secs. VI–IX, we need only the order of these functions but not their explicit form. In Eqs. (18–23) we used the absolute value of $\Psi''(\Phi_0)$, which happens to be strictly negative at the SIP [see Eq. (8)]. We made no assumptions, however, about the sign of the third derivative of $\Psi(\phi)$ at the SIP. Thus, we would like to stress that, with the possible exception of c_2 and c_3, all of the constants defined in Eqs. (21–23) are strictly positive. In the stability analysis that follows it will be important to remember that Eqs. (18–20) still represent the complete MG, namely, they are equivalent to Eqs. (13–15), which are in turn equivalent to Eqs. (1–3) and (10). Thus, although our stability

analysis is a local one, our results will be valid for the full MG and not for any approximation of it. During our analysis we will also need the following. First, by introducing the transformation

$$y_3 = x_3^p, \qquad \mathrm{d}y_3 = p x_3^{p-1}\,\mathrm{d}x_3 \tag{24}$$

the system of Eqs. (18–20) can be written in the equivalent form

$$\frac{\mathrm{d}x_1}{\mathrm{d}t} = -a_1 x_2 - a_2 x_1^2 - a_3 y_3^{2/p} + \delta^3 f_1\left(x_1, y_3^{1/p}\right) \tag{25}$$

$$\frac{\mathrm{d}x_2}{\mathrm{d}t} = b_1 x_1 - b_2 x_2 - (u_d + k y_3)\left[b_3 - \delta^1 f_{21}(x_2)\right] + \delta^2 f_{22}(x_2) \tag{26}$$

$$\frac{\mathrm{d}y_3}{\mathrm{d}t} = p y_3\left[-c_1 x_1 + c_2 y_3^{2/p} + c_3 x_1^2 + \delta^3 f_3\left(x_1, y_3^{1/p}\right)\right] \tag{27}$$

We will need this version of the MG whenever we linearize about an equilibrium with $0 < p \leq 1$. Second, from Eq. (20), if x_3 is zero at any time, then x_3 must be identically zero in $-\infty < t < \infty$. Thus, 1) the trajectory of the system of Eqs. (18–20) cannot cross over the $x_3 = 0$ plane, so that with no loss of generality x_3 can always be taken as nonnegative, and 2) if x_3 is nonzero at any time, then in the ensuing time evolution of the system of Eqs. (18–20), x_3 can go to zero only asymptotically with t. Similar statements also apply to Eqs. (25–27).

VI. Branching of Equilibria from the SIP

We now examine how the equilibria bifurcate from the SIP when the control S [see Eq. (17)] contains a nonzero, infinitesimal, throttle disturbance u_d. The equilibrium is at the SIP only when u_d is zero. When u_d is nonzero, the equilibrium is determined by setting the right-hand sides of Eqs. (18–20) equal to zero. Let x_{1e}, x_{2e}, and x_{3e} denote the equilibrium values of x_1, x_2, and x_3, respectively, when u_d is nonzero. Then, from Eq. (20), we see that there are two possibilities. The first corresponds to setting $x_{3e} = 0$, in which case, a simple inspection of the right-hand sides of Eqs. (18) and (19) reveals that for very small u_d the equilibrium is given by

$$x_{1e} = b_3 u_d / b_1 + \mathcal{O}\left(u_d^2\right), \qquad x_{2e} = -a_2 x_{1e}^2 / a_1 + \mathcal{O}\left(x_{1e}^3\right)$$
$$x_{3e} = 0 \tag{28}$$

where, $\mathcal{O}(\ )$ denotes the (higher-) order symbol. This results in the AB (see Fig. 3). The second possibility leads to the NAB (see Fig. 3) and arises when

$$-c_1 x_{1e} + c_2 x_{3e}^2 + c_3 x_{1e}^2 + \delta^3 f_3(x_{1e}, x_{3e}) = 0 \tag{29}$$

In this case, the right-hand side of Eq. (20) is again zero. For infinitesimally small u_d, Eq. (29) balances if

$$x_{1e} = c_2 x_{3e}^2 / c_1 + \mathcal{O}\left(x_{3e}^3\right) \tag{30}$$

From Eq. (30) and the right-hand side of Eq. (18), a similar inspection shows that along such equilibria

$$x_{2e} = -a_3 x_{3e}^2 / a_1 + \mathcal{O}\left(x_{3e}^3\right) \tag{31}$$

Combining Eqs. (30) and (31) with the fact that for such equilibria the right-hand-side of Eq. (19) must also be zero, we conclude that for very small u_d the NAB is locally fixed by

$$u_d = -k x_{3e}^p + k_{\mathrm{crit}} x_{3e}^2 + \mathcal{O}\left(x_{3e}^{p+1}, x_{3e}^3\right) \tag{32}$$

where k_{crit} is just a constant given by

$$k_{\mathrm{crit}} = (1/b_3)(b_1 c_2 / c_1 + b_2 a_3 / a_1) \tag{33}$$

Using Eqs. (21–23), we find that k_{crit} can be written in terms of more direct compressor parameters as

$$k_{\mathrm{crit}} = \frac{S_0}{8\Phi_0 |\Psi''(\Phi_0)|}\left[\Psi'''(\Phi_0) + \frac{S_0^2 [\Psi''(\Phi_0)]^2}{\Phi_0}\right] \tag{34}$$

Depending on k and p, there can be three types of NAB (bifurcations) for arbitrarily small u_d. These, as well as the AB, are shown qualitatively on a x_{3e} vs u_d diagram in Figs. 4–7. Dashed lines show unstable equilibria, whereas solid lines show asymptotically stable equilibria. When $k = 0$, or when $k > 0$ and $p > 2$, feedback has no effect on the branching of equilibria. In this case, Eq. (32) becomes

$$u_d = k_{\mathrm{crit}} x_{3e}^2 + \mathcal{O}\left(x_{3e}^3\right) \tag{35}$$

In practice, for a compressor exhibiting the RS instability, k_{crit} is strictly positive. Then, as shown in Fig. 4, the bifurcation at SIP is of the subcritical pitchfork type. When $k > 0$ and $p = 2$, namely, for quadratic feedback, the qualitative features of the NAB depend strongly on whether $k > k_{\mathrm{crit}}$ or $k < k_{\mathrm{crit}}$,

$$u_d = -(k - k_{\mathrm{crit}}) x_{3e}^2 + \mathcal{O}\left(x_{3e}^3\right) \tag{36}$$

In this case, the bifurcation is of the subcritical pitchfork type for $k < k_{\mathrm{crit}}$ (same as in Fig. 4) and of the supercritical pitchfork type when $k > k_{\mathrm{crit}}$ (as in Fig. 5). For $k = k_{\mathrm{crit}}$, higher-order terms must be examined to determine the type of the bifurcation. We will set

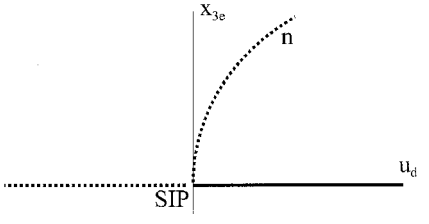

Fig. 4 Qualitative bifurcation diagram near the SIP under no feedback control ($k = 0$).

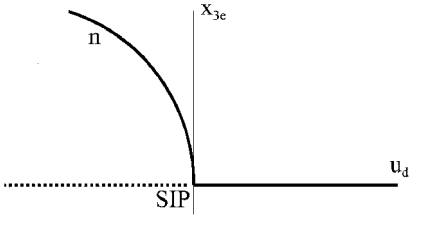

Fig. 5 Qualitative bifurcation diagram near the SIP under quadratic ($p = 2$) feedback with $k > k_{\mathrm{crit}}$.

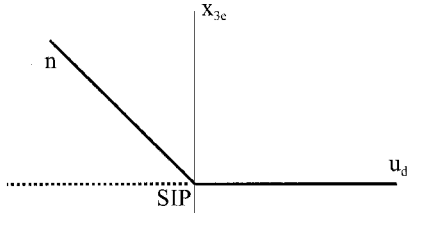

Fig. 6 Qualitative bifurcation diagram near the SIP under linear feedback ($k > 0$ and $p = 1$).

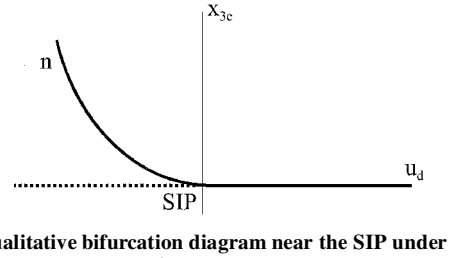

Fig. 7 Qualitative bifurcation diagram near the SIP under sublinear feedback ($k > 0$ and $0 < p < 1$).

aside that case because it is practically uninteresting. When $k > 0$ and $0 < p < 2$, the quadratic term in Eq. (32) is subdominant, and the bifurcation is locally described by

$$u_d = -kx_{3e}^p + \mathcal{O}\left(x_{3e}^{p+1}, x_{3e}^2\right) \tag{37}$$

Now, for $k > 0$ and $1 < p < 2$, the bifurcation is still of the supercritical pitchfork type, and the NAB is perpendicular to the AB at SIP (just as in Fig. 5). For $k > 0$ and $p = 1$, on the other hand, the bifurcation changes to a transcritical one, as shown in Fig. 6. Finally, for $k > 0$ and $0 < p < 1$, the NAB is tangent to the AB at SIP as shown in Fig. 7. In this case, although different than that in Fig. 6, the bifurcation is still of the transcritical type. The local stability of equilibria shown in Figs. 4–7 will be analyzed in Sec. IX.

VII. End Result

Before proceeding further we will provide a useful road map by collecting together and stating clearly all of the details that we will prove in Secs. VIII and IX. These are valid for the full MG and for an arbitrary compressor map [Eqs. (1–3) and (10), or Eqs. (13–15), or Eqs. (18–20), or Eqs. (25–27)]. The critical gain of the system, k_{crit}, is defined in Eqs. (33) and (34). By feedback we refer to the control term kA^p. The first four points are valid under no persistent throttle disturbance ($u_d = 0$) and pertain to the local stability of the SIP.

1) When the feedback is off ($k = 0$), the SIP for the corresponding uncontrolled system is locally asymptotically stable if $k_{\text{crit}} < 0$ and unstable if $k_{\text{crit}} > 0$ (Sec. VIII.A).

2) Under quadratic feedback ($k > 0$ and $p = 2$), the SIP is locally asymptotically stable if $k > k_{\text{crit}}$ and unstable if $k < k_{\text{crit}}$ (Sec. VIII.B).

3) Feedback control with $k > 0$ and $p > 2$ has no effect on the local stability of the SIP. Under such control the SIP is locally asymptotically stable if $k_{\text{crit}} < 0$ and unstable if $k_{\text{crit}} > 0$ (Sec. VIII.C).

4) Under feedback control with $k > 0$ and $0 < p < 2$, the SIP is locally asymptotically stable for any value of k (Sec. VIII.D).

The next five points are valid for operation under a persistent, infinitesimally small, throttle disturbance u_d, and they pertain to the local stability of the axisymmetric (AB) and nonaxisymmetric (NAB) branches bifurcating from the SIP. Φ_e here refers to the value of Φ at the corresponding equilibrium.

5) Throttle feedback control has no effect on the local stability of an equilibrium lying on the AB. Such an equilibrium is locally asymptotically stable if $\Psi'(\Phi_e) < 0$ and unstable if $\Psi'(\Phi_e) > 0$ (Sec. IX.A).

6) For the uncontrolled system ($k = 0$) an equilibrium lying on the NAB is locally asymptotically stable if $k_{\text{crit}} < 0$ and unstable if $k_{\text{crit}} > 0$ (Sec.IX.B).

7) Under quadratic feedback ($k > 0$ and $p = 2$), an equilibrium lying on the NAB is locally asymptotically stable if $k > k_{\text{crit}}$ and unstable if $k < k_{\text{crit}}$ (Sec. IX.B).

8) Feedback control with $k > 0$ and $p > 2$ has no effect on the local stability of an equilibrium lying on the NAB. Under such control such an equilibrium is locally asymptotically stable if $k_{\text{crit}} < 0$ and unstable if $k_{\text{crit}} > 0$ (Sec. IX.B).

9) Under feedback control with $k > 0$ and $0 < p < 2$, an equilibrium lying on the NAB is locally asymptotically stable for any value of k. Moreover, for $0 < p < 1$, the NAB is tangent to the AB at the SIP. Thus, in this case, the NAB locally mimics the stable part of the AB at the SIP (Sec. IX.B).

Note that points 1, 5, and 6 are well known, whereas points 2 and 7 have been partially addressed and uncovered in previous work.[7,8] Points 3, 4, 8, and 9 on the other hand represent our primary contribution.

VIII. Stability for Operation at the SIP

We will first assume that in Eqs. (18–20) u_d is zero and perform a complete ($k \geq 0$ and $p > 0$) local stability analysis for the SIP. For the uncontrolled system ($k = 0$), and for $k > 0$ and $p \geq 2$, we will use the center manifold (CM) theory. For $k > 0$ and $0 < p < 2$, on the other hand, we will resort to Lyapunov's direct method. The reader is referred to Verhulst,[13] Perko,[14] and Guckenheimer and Holmes[15] for the underlying theory.

Let us start by linearizing the MG about the SIP. We must be careful to distinguish between two cases. If $p > 1$, then we linearize the system of Eqs. (18–20), whereas if $0 < p \leq 1$, then we linearize the equivalent system of Eqs. (25–27). We find that in both cases the linearized system is governed by a Jacobian matrix given by

$$J_0 = \begin{bmatrix} 0 & -a_1 & 0 \\ b_1 & -b_2 & J_{230} \\ 0 & 0 & 0 \end{bmatrix} \tag{38}$$

where the term $J_{230} = 0$ when $p > 1$ and $J_{230} = -kb_3$ when $0 < p \leq 1$. Both cases lead to the characteristic equation

$$\lambda^3 + \eta_0\lambda^2 + \mu_0\lambda + \nu_0 = 0 \tag{39}$$

whose coefficients are given by

$$\eta_0 = b_2, \qquad \mu_0 = a_1 b_1, \qquad \nu_0 = 0 \tag{40}$$

Because $\nu_0 = 0$, whereas η_0 and μ_0 are strictly positive, two eigenvalues have negative real parts and one eigenvalue is zero. Thus, the linearized approximation does not determine the stability of the full nonlinear system. Because no eigenvalue has a strictly positive real part, the flow of the system of Eqs. (18–20) exhibits stable behavior near the SIP, except perhaps in the CM.[13–15] In this case the CM is one dimensional. If we can find a local approximation for the CM, valid near the SIP, we only need to study the flow locally in the CM to study the local stability of the SIP.[13–15] For $k = 0$ (no feedback) or $k > 0$ and $p \geq 2$, this is relatively straightforward. With no loss of generality the CM is taken as

$$x_1 = h(x_3) = h_1(x_3) + x_3^p h_2(x_3) \tag{41}$$

$$x_2 = w(x_3) = w_1(x_3) + x_3^p w_2(x_3) \tag{42}$$

where h, w, h_1, h_2, w_1, and w_2 are functions of x_3, with $h(0) = w(0) = 0$, to be determined so that Eqs. (18) and (19) are identically satisfied. To uncover the local behavior of these functions about the SIP, we assume power series expansions, substitute in Eqs. (18) and (19), use Eq. (20) for the time derivative of x_3, and match terms. This works only when the CM is analytic at SIP, namely,[13–15] only when such an expansion about the SIP exists.

A. Stability of the Uncontrolled System ($k = 0$)

In this case, the feedback is off and the CM near the SIP is approximated as

$$x_1 = h(x_3) = -(b_2a_3/b_1a_1)x_3^2 + \mathcal{O}\left(x_3^3\right) \tag{43}$$

$$x_2 = w(x_3) = -(a_3/a_1)x_3^2 + \mathcal{O}\left(x_3^3\right) \tag{44}$$

The local behavior of the flow in the CM is obtained by substituting from Eqs. (43) and (44) into Eq. (20),

$$\frac{\mathrm{d}x_3}{\mathrm{d}t} = \left(\frac{c_1b_3k_{\text{crit}}}{b_1}\right)x_3^3 + \mathcal{O}\left(x_3^4\right) \tag{45}$$

where k_{crit} was defined in Eq. (33). The coefficient c_1b_3/b_1 is strictly positive, and so the SIP for the uncontrolled system is locally asymptotically stable if $k_{\text{crit}} < 0$ and unstable if $k_{\text{crit}} > 0$. This proves point 1 of Sec. VII.

B. Stability Under Quadratic Feedback ($k > 0$ and $p = 2$)

In this case, the CM near the SIP is found as

$$x_1 = h(x_3) = (b_3k/b_1 - b_2a_3/b_1a_1)x_3^2 + \mathcal{O}\left(x_3^3\right) \tag{46}$$

$$x_2 = w(x_3) = -(a_3/a_1)x_3^2 + \mathcal{O}\left(x_3^3\right) \tag{47}$$

whereas the flow in the CM near the SIP obeys

$$\frac{dx_3}{dt} = -\left(\frac{c_1 b_3}{b_1}\right)(k - k_{crit})x_3^3 + \mathcal{O}(x_3^4) \tag{48}$$

Thus, the SIP is locally asymptotically stable if $k > k_{crit}$ and unstable if $k < k_{crit}$. This proves point 2 of Sec. VII.

C. Stability for $k > 0$ and $p > 2$: Control Effectiveness

In this case, feedback has no effect on the local stability of the SIP. The CM is given by expressions identical to Eqs. (43) and (44). The difference is that the higher-order terms are of order p if $2 < p < 3$. The flow in the CM is locally described by a differential equation identical to Eq. (45), the difference again being that the higher-order terms are of order $p + 1$ if $2 < p < 3$. Thus, under feedback with $k > 0$ and $p > 2$, the SIP is locally asymptotically stable if $k_{crit} < 0$ and unstable if $k_{crit} > 0$. This proves point 3 of Sec. VII.

D. Stability for $k > 0$ and $0 < p < 2$

In this case we will use Lyapunov's direct method rather than the CM theory to show the stability of the SIP. To ease the analysis, we first transform from the variables x_1, x_2, x_3, and t to a new set ξ_1, ξ_2, ξ_3, and τ,

$$\tau = b_2 t, \qquad \xi_1 = (pc_1/b_2)x_1 \tag{49}$$

$$\xi_2 = \left(pa_1c_1/b_2^2\right)x_2, \qquad \xi_3 = \left(pka_1b_3c_1/b_2^3\right)x_3^p \tag{50}$$

Then Eqs. (18–20) assume the following equivalent form:

$$\frac{d\xi_1}{d\tau} = -\xi_2 - \alpha_1\xi_1^2 - \alpha_2\xi_3^{2/p} + \delta^3 g_1\left(\xi_1, \xi_3^{1/p}\right) \tag{51}$$

$$\frac{d\xi_2}{d\tau} = \beta\xi_1 - \xi_2 - \xi_3 + \xi_3\delta^1 g_{21}(\xi_2) + \delta^2 g_{22}(\xi_2) \tag{52}$$

$$\frac{d\xi_3}{d\tau} = \xi_3\left[-\xi_1 + \gamma_1\xi_3^{2/p} + \gamma_2\xi_1^2 + \delta^3 g_3\left(\xi_1, \xi_3^{1/p}\right)\right] \tag{53}$$

where the constants α_1, α_2, β, γ_1, and γ_2 are defined as

$$\alpha_1 = \frac{a_2}{pc_1}, \qquad \alpha_2 = \left(\frac{a_3^p b_2^{6-2p}}{p^{2-p}k^2a_1^2b_3^2c_1^{2-p}}\right)^{1/p} \tag{54}$$

$$\beta = \frac{a_1b_1}{b_2^2}, \qquad \gamma_1 = \left(\frac{b_2^{6-p}c_2^p}{p^{2-p}k^2a_1^2b_3^2c_1^2}\right)^{1/p}, \qquad \gamma_2 = \frac{b_2c_3}{pc_1^2} \tag{55}$$

The δg terms in Eqs. (51–53) correspond to the δf terms of Eqs. (18–20). For $0 < p < 2$, all of these terms are of higher order in the variables ξ_1, ξ_2, and ξ_3 than the terms shown explicitly. Consider now a function L, defined as

$$L(\xi_1, \xi_2, \xi_3) = \xi_3 + \frac{1}{2}\sum_{i=1}^{2}\left(D_i\xi_1 + \frac{\xi_2}{2} + C_i\xi_3\right)^2 \tag{56}$$

where D_i and C_i, $i = 1, 2$, are constants given by

$$D_1 = \frac{-1 + \sqrt{1 + 4\beta}}{4}, \qquad C_1 = \frac{-4\beta - 3 + 3\sqrt{1 + 4\beta}}{4\beta\sqrt{1 + 4\beta}} \tag{57}$$

$$D_2 = \frac{-1 - \sqrt{1 + 4\beta}}{4}, \qquad C_2 = \frac{4\beta + 3 + 3\sqrt{1 + 4\beta}}{4\beta\sqrt{1 + 4\beta}} \tag{58}$$

The time derivative of L, along a trajectory of the system of Eqs. (51–53), can be found by differentiating the right-hand side of Eq. (56) with respect to τ and by substituting from Eqs. (51–53). The result is

$$\frac{dL}{d\tau} = -\frac{\beta}{4}\xi_1^2 - \frac{1}{4}\xi_2^2 - \frac{3}{4\beta}\xi_3^2 + \text{HOT} \tag{59}$$

where with HOT we refer to terms that are (for $0 < p < 2$) of higher order than the second. Note that the δg terms in Eqs. (51–53) contribute only to the HOT part of $dL/d\tau$. Hence, they have no effect on the local behavior of $dL/d\tau$ near the SIP. From Eq. (59) this local behavior is seen to be rather simple: Because β is strictly positive, $dL/d\tau$ is locally negative definite about the SIP. More precisely, the following may be said about L

F1) $L(\xi_1, \xi_2, \xi_3)$ is strictly positive for strictly positive ξ_3 and positive definite for $\xi_3 = 0$.

F2) For $L_0 > 0$ sufficiently small, in the (ξ_1, ξ_2, ξ_3) state space there exists a compact region B defined by $L(\xi_1, \xi_2, \xi_3) \le L_0$ and $\xi_3 \ge 0$, so that $dL/d\tau$ is zero at $(\xi_1, \xi_2, \xi_3) = (0, 0, 0)$ and strictly negative at any other point in B. To this we add the details on x_3 supplied in Sec. V, given now in terms of the variable ξ_3.

F3) From Eq. (53), if ξ_3 is zero at any time, then ξ_3 must be identically zero in $-\infty < \tau < \infty$. Namely, the trajectory of the system of Eqs. (51–53) cannot cross over $\xi_3 = 0$, and so with no loss of generality, $\xi_3 \ge 0$ always.

F4) If $\xi_3 > 0$ at any τ, then in the ensuing evolution of Eqs. (51–53) ξ_3 can go to zero only asymptotically with τ.

We can now show that the SIP is locally asymptotically stable. Consider the behavior, of any trajectory of the system of Eqs. (51–53), as τ tends to infinity, that starts from within the region B (the existence of which is guaranteed by item F2), with a nonnegative ξ_3. Then from item F3, only one among the following is true:

1) The starting value of ξ_3 is zero.

2) The starting value of ξ_3 is strictly positive.

If item 1 is true, then from item F3, ξ_3 stays identically at zero, whereas from items F1 and F2 the rest of the system asymptotically goes to the SIP. If item 2 is true, then from items F3 and F4 ξ_3 stays strictly positive for any finite τ. In this case, from items F1 and F2 the whole system asymptotically goes to the SIP. Therefore, for $0 < p < 2$ the SIP is locally asymptotically stable for any strictly positive value of k. This proves point 4 of Sec. VII.

IX. Stability Under a Persistent Throttle Disturbance

We will now perform a complete ($k \ge 0$ and $p > 0$) local stability analysis for the equilibria on the AB and NAB near the SIP (small u_d). As in Sec. VI, we denote all of these equilibria using the subscript e. We will use linearization of the MG about such equilibria. The characteristic equation for the linearized system will have no eigenvalues lying on the imaginary axis, and so such linearization will be sufficient to determine stability.

A. Stability of the Axisymmetric Branch (AB)

From Eqs. (13–15) the conditions for an equilibrium on the AB are

$$A_e = 0, \qquad \Delta P_e = \Psi(\Phi_e), \qquad \Phi_e = S_e\sqrt{\Delta P_e}, \qquad S_e = S_0 + u_d \tag{60}$$

We must distinguish between two cases. When $p > 1$, we linearize Eqs. (13–15) directly about the equilibrium. When, on the other hand, $0 < p \le 1$, then the feedback term kA^p in Eq. (14) cannot be linearized about $A_e = 0$. In this case, we use the transformation $E = A^p$ and linearize the transformed system,

$$\frac{d\Phi}{dt} = -\frac{\Delta P}{m} + \frac{1}{m}\sum_{\kappa=0}^{\infty}\frac{\Psi^{2\kappa}(\Phi)}{(\kappa!)^2}\left(\frac{E^{1/p}}{2}\right)^{2\kappa} \tag{61}$$

$$\frac{d(\Delta P)}{dt} = \frac{1}{V}\left[\Phi - (S_0 + u_d + kE)\sqrt{\Delta P}\right] \tag{62}$$

$$\frac{dE}{dt} = pME\sum_{\kappa=1}^{\infty}\frac{\kappa\Psi^{2\kappa-1}(\Phi)}{2(\kappa!)^2}\left(\frac{E^{1/p}}{2}\right)^{2\kappa-2} \tag{63}$$

about the equilibrium. In both cases the Jacobian matrix associated with the linearized system is expressed as

$$J_e = \begin{bmatrix} \Psi'(\Phi_e)/m & -(1/m) & 0 \\ 1/V & -\left(S_e^2/2V\Phi_e\right) & J_{23e} \\ 0 & 0 & J_{33e} \end{bmatrix} \tag{64}$$

where $J_{23e}=0$ when $p>1$ and $J_{23e}=-(k\Phi_e/VS_e)$ when $0<p\leq 1$. Also, $J_{33e}=M\Psi'(\Phi_e)/2$ when $p>1$, and $J_{33e}=pM\Psi'(\Phi_e)/2$ when $0<p\leq 1$. The associated characteristic equation has a root at $\lambda=J_{33e}$. Its other two roots are found from

$$\lambda^2+\left[\frac{S_e^2}{2V\Phi_e}-\frac{\Psi'(\Phi_e)}{m}\right]\lambda+\frac{1}{mV}-\frac{S_e^2\Psi'(\Phi_e)}{2mV\Phi_e}=0 \tag{65}$$

For $\Psi'(\Phi_e)<0$, all three roots have strictly negative real parts. For $\Psi'(\Phi_e)>0$, at least one root has a strictly positive real part. Moreover, this condition does not depend on k. This proves point 5 of Sec. VII.

B. Stability of the Nonaxisymmetric Branch (NAB)

To determine the stability of the NAB we proceed as follows. The linearized approximation of the MG about an equilibrium on the NAB is governed by a Jacobian matrix J_e and a characteristic equation:

$$\lambda^3+\eta_e\lambda^2+\mu_e\lambda+\nu_e=0 \tag{66}$$

The coefficients of this equation are continuous functions of u_d. For $u_d=0$, the equilibrium is at the SIP, and these coefficients are given by Eq. (40). For infinitesimally small u_d, the same coefficients are perturbed to

$$\eta_e=b_2+\delta\eta, \qquad \mu_e=a_1b_1+\delta\mu, \qquad \nu_e=\delta\nu \tag{67}$$

with $\delta\eta$, $\delta\mu$, and $\delta\nu$ denoting infinitesimal perturbations. Because $b_2>0$ and $a_1b_1>0$, it follows that $\eta_e>0$ and $\mu_e>0$ for sufficiently small u_d. The first column of the corresponding Routh table (see Ref. 16) implies that the necessary and sufficient conditions for stability are $\eta_e>0$ and $\nu_e>0$ and $(\eta_e\mu_e-\nu_e)/\eta_e>0$. Because $\eta_e>0$ and $\mu_e>0$ and ν_e is infinitesimal, these conditions are satisfied if and only if $\nu_e>0$. Thus, we only need to check the sign of ν_e. Note that ν_e is just the negative of the determinant of the Jacobian matrix J_e,

$$\nu_e=-\det(J_e) \tag{68}$$

To obtain $\det(J_e)$ write Eqs. (13–15) by condensing the MG integrals [see Eqs. (11) and (12)]:

$$\frac{d\Phi}{dt}=\frac{1}{m}[F(\Phi,A)-\Delta P] \tag{69}$$

$$\frac{d(\Delta P)}{dt}=\frac{1}{V}\left[\Phi-\left(S_0+u_d+kA^p\right)\sqrt{\Delta P}\right] \tag{70}$$

$$\frac{dA}{dt}=MG(\Phi,A) \tag{71}$$

An equilibrium on the NAB satisfies

$$G(\Phi_e,A_e)=0, \qquad \Delta P_e=F(\Phi_e,A_e), \qquad \Phi_e=S_e\sqrt{\Delta P_e} \tag{72}$$

$$S_e=S_0+u_d+kA_e^p \tag{73}$$

For compatibility with the linearization about the SIP [Eqs. (38–40)], we have to distinguish between the cases $p>1$ and $0<p\leq 1$. When $p>1$, linearization of Eqs. (69–71) about such an equilibrium results in

$$J_e=\begin{bmatrix} \frac{1}{m}\left(\frac{\partial F}{\partial\Phi}\right)_e & -\left(\frac{1}{m}\right) & \frac{1}{m}\left(\frac{\partial F}{\partial A}\right)_e \\ \frac{1}{V} & -\frac{S_e^2}{2V\Phi_e} & -\frac{kpA_e^{p-1}\Phi_e}{VS_e} \\ M\left(\frac{\partial G}{\partial\Phi}\right)_e & 0 & M\left(\frac{\partial G}{\partial A}\right)_e \end{bmatrix} \tag{74}$$

When $0<p\leq 1$, Eqs. (69–71) are transformed through $E=A^p$. Linearization then yields a similar Jacobian that we denote by I_e. It can be checked that J_e and I_e differ only in their third column. The third column of I_e is equal to the third column of J_e, multiplied by the factor

$$\left(\frac{dA}{dE}\right)_e=\frac{A_e^{1-p}}{p} \tag{75}$$

Because this factor is strictly positive, the determinants of J_e and I_e have the same sign. Thus, we only need one of them to determine the sign of ν_e. Instead of ν_e we will check the sign of a similar constant, N_e, defined as

$$N_e=\left(\frac{2mVS_e\Phi_e}{M}\right)\nu_e=-\left(\frac{2mVS_e\Phi_e}{M}\right)\det(J_e) \tag{76}$$

Clearly, N_e and ν_e have the same sign. Expanding the determinant of J_e in Eq. (74) we obtain

$$N_e=(F_\Phi G_A-F_A G_\Phi)S_e^3-2pkA_e^{p-1}G_\Phi\Phi_e^2-2G_AS_e\Phi_e \tag{77}$$

where

$$F_\Phi=\left(\frac{\partial F}{\partial\Phi}\right)_e, \qquad G_A=\left(\frac{\partial G}{\partial A}\right)_e$$

$$F_A=G_\Phi=\left(\frac{\partial F}{\partial A}\right)_e=\left(\frac{\partial G}{\partial\Phi}\right)_e \tag{78}$$

That $F_A=G_\Phi$ is shown in Appendix B. For an equilibrium on the NAB, Eqs. (16) and (17) read

$$\Phi_e=\Phi_0+x_{1e}, \qquad \Delta P_e=\Delta P_0+x_{2e}, \qquad A_e=x_{3e} \tag{79}$$

$$S_e=S_0+u_d+kx_{3e}^p \tag{80}$$

where x_{1e}, x_{2e}, x_{3e}, and u_d are not independent, but vary according to Eqs. (30–32). If we expand N_e [Eq. (77)] in x_{3e} about the SIP, the lowest-order terms of such an expansion will reveal the sign of N_e for infinitesimally small u_d. The partial derivatives of F and G with respect to A and Φ expand about the SIP as

$$F_\Phi=\left(\frac{\partial F}{\partial\Phi}\right)_e=-|\Psi''(\Phi_0)|x_{1e}+\frac{\Psi'''(\Phi_0)}{4}x_{3e}^2+\text{HOT} \tag{81}$$

$$G_A=\left(\frac{\partial G}{\partial A}\right)_e=-\frac{|\Psi''(\Phi_0)|}{2}x_{1e}+\frac{3\Psi'''(\Phi_0)}{16}x_{3e}^2+\text{HOT} \tag{82}$$

$$F_A=G_\Phi=\left(\frac{\partial F}{\partial A}\right)_e=\left(\frac{\partial G}{\partial\Phi}\right)_e=-\frac{|\Psi''(\Phi_0)|}{2}x_{3e}+\text{HOT} \tag{83}$$

On the NAB, x_{1e} and x_{3e} are related by Eq. (30). By substitution into Eqs. (81–83), we find

$$F_\Phi G_A-F_AG_\Phi=-\left\{[\Psi''(\Phi_0)]^2/4\right\}x_{3e}^2+\text{HOT} \tag{84}$$

Finally, from Eqs. (79), (80), (84), and (77), for an equilibrium on the NAB arbitrarily close to the SIP, N_e is

$$N_e = 2|\Psi''(\Phi_0)|\Phi_0^2\left[(pk/2)x_{3e}^p - k_{\text{crit}}x_{3e}^2\right] + \text{HOT} \tag{85}$$

Here k_{crit} is the constant defined in Eqs. (33) and (34). Recalling that an equilibrium on the NAB arbitrarily close to the SIP is locally asymptotically stable if and only if $N_e > 0$, we have, depending on k, p, four possible cases.

1) For the uncontrolled system ($k = 0$), N_e becomes

$$N_e = -2|\Psi''(\Phi_0)|\Phi_0^2 k_{\text{crit}}x_{3e}^2 + \text{HOT} \tag{86}$$

Locally N_e has opposite sign than k_{crit}. Thus, in this case, an equilibrium lying on the NAB is locally asymptotically stable if $k_{\text{crit}} < 0$ and unstable if $k_{\text{crit}} > 0$. This proves point 6 of Sec. VII.

2) Under quadratic feedback ($k > 0$ and $p = 2$), N_e becomes

$$N_e = 2|\Psi''(\Phi_0)|\Phi_0^2(k - k_{\text{crit}})x_{3e}^2 + \text{HOT} \tag{87}$$

In this case an equilibrium lying on the NAB is locally asymptotically stable if $k > k_{\text{crit}}$ and unstable if $k < k_{\text{crit}}$. This proves point 7 of Sec. VII.

3) When $k > 0$ and $p > 2$, locally the feedback term has no effect on N_e. Namely, N_e behaves as in Eq. (86). Under such control, an equilibrium lying on the NAB is locally asymptotically stable if $k_{\text{crit}} < 0$ and unstable if $k_{\text{crit}} > 0$. This proves point 8 of Sec. VII.

4) When $k > 0$ and $0 < p < 2$, then N_e behaves as

$$N_e = |\Psi''(\Phi_0)|\Phi_0^2 pkx_{3e}^p + \text{HOT} \tag{88}$$

Under such control an equilibrium lying on the NAB is locally asymptotically stable for any value of k. Combined with Fig. 7 this proves point 9 of Sec. VII.

X. Unifying Geometric Explanation

The results of Sec. VII can be unified under a single geometric picture. Recall (Sec. III) that varying S does not affect the shape of the USB or SB (Fig. 2). These are fixed by the right-hand sides of Eqs. (1) and (3). Varying S does affect, however, the equilibrium implied by Eq. (2). For a control of the type we considered [see Eqs. (10) and (17)], this condition reads

$$\Phi_0 + x_{1e} = \left(S_0 + u_d + kx_{3e}^p\right)\sqrt{\Delta P_0 + x_{2e}} \tag{89}$$

In the absence of RS, x_{3e} is identically zero and the operating point lies on the USB. From Sec. IX.A, both the shape and the stability of points (other than points b and s in Fig. 2) on the USB remains unchanged by any type of throttle control. Thus, locally, near the SIP, the USB always looks like the branch usv in Fig. 8 [see second of Eqs. (28)]. The SB, on the other hand, locally, is just a straight line, which from Eqs. (30) and (31) is found as

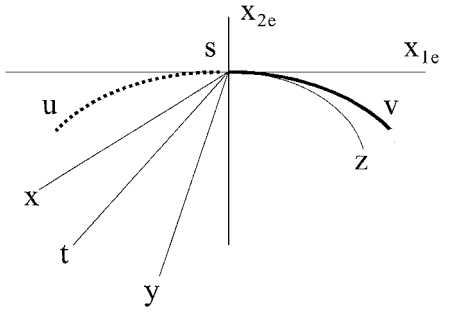

Fig. 8 Qualitative locus of unstalled (usv) and stalled (st) branches of equilibria near the SIP, together with three different types (sx, sy, and sz) of feedback throttle characteristics.

$$x_{1e} = -\frac{a_1 c_2}{a_3 c_1}x_{2e} = -\frac{\Psi'''(\Phi_0)}{2[\Psi''(\Phi_0)]^2}x_{2e} \tag{90}$$

This is shown by the straight line st in Fig. 8. Contrary to the USB, the stability of operating points on the SB is strongly affected by the particular type of throttle control. Keeping first-order terms in the small quantities x_{ie} and u_d, locally about the SIP Eq. (89) can be written as

$$x_{1e} = \left(S_0^2/2\Phi_0\right)x_{2e} + (k\phi_0/S_0)x_{3e}^p + (\Phi_0/S_0)u_d \tag{91}$$

For operation on the SB, one can eliminate x_{3e} by relating it to x_{2e} through Eq. (31). Then, Eq. (91) becomes

$$x_{1e} = \frac{S_0^2}{2\Phi_0}x_{2e} + \frac{2^p k\Phi_0}{S_0|\Psi''(\Phi_0)|^{p/2}}(-x_{2e})^{p/2} + \frac{\Phi_0}{S_0}u_d \tag{92}$$

Equation (92) can be viewed as a local feedback throttle characteristic (LFTC). In the $x_{1e}x_{2e}$ plane for $u_d = 0$, the LFTC passes through the SIP. When $u_d < 0$, then the LFTC shifts to the left. Figure 8 shows the shapes of the LFTC for all cases of feedback and for $u_d = 0$. When $p > 2$, or $k = 0$, locally, the first term on the right-hand side of Eq. (92) is dominant, and the LFTC is a straight line, such as line sx or sy. Points 1, 3, 6, and 8 of Sec. VII lead to the stability requirement that the inclination of this line relative to the x_{2e} axis be less than the corresponding inclination of line st. Thus, an LFTC of the form sx implies instability, whereas an LFTC of the form sy implies stability. When $k > 0$ and $p = 2$, the LFTC is still a straight line, such as line sx or sy, but now the first two terms on the right-hand side of Eq. (92) are of equal importance. Now, points 2 and 7 of Sec. VII lead to the same conclusion, namely, that an LFTC of the form sx implies instability, whereas an LFTC of the form sy implies stability. When on the other hand $k > 0$ and $0 < p < 2$, then only the second term on the right-hand side of Eq. (92) is locally dominant, and the LFTC looks like the curve sz in Fig. 8. Now, points 4 and 9 of Sec. VII imply stability for all such LFTCs. As u_d shifts infinitesimally from $u_d = 0$ to $u_d < 0$, the LFTCs sx, sy, and sz in Fig. 8 shift infinitesimally to the left. After such a shift only the LFTCs sy and sz still intersect the local part (line st) of the SB. This leads to a general statement connecting all of the results of Sec. VII to the behavior of the LFTC: The feedback control law defined in Eqs. (10) and (17) locally asymptotically stabilizes the SIP and the neighboring part of the SB if and only if it results in an LFTC for which the jump (in the ΔP vs Φ plane of equilibria) that leads to finite amplitude RS when S is reduced below its value at the SIP is eliminated. The rate at which the LFTC sweeps by the SB for decreasing, negative u_d determines the shape of the NAB and the types of the corresponding bifurcations in Figs. 4–7.

XI. Conclusions

We presented a complete, analytical, local stability analysis for the Moore–Greitzer model of compressor rotating stall about the stall inception point and the neighboring part of the branch of the axisymmetric and nonaxisymmetric bifurcated equilibria. Our analysis is valid for all throttle feedback control laws that are equal to the rotating stall amplitude, raised to a strictly positive feedback exponent, and multiplied by a nonnegative feedback gain. We showed that linear feedback reshapes and stabilizes the neighboring nonaxisymmetric branch and results in unconditional local asymptotic stability for the stall inception point. Quadratic feedback on the other hand represents a limiting case of local control effectiveness and at best leads to conditional local stability, that is, it renders the stall inception point and the neighboring nonaxisymmetric branch locally asymptotically stable only for sufficiently high values of the feedback gain. Our most important result is perhaps that sublinear feedback, that is, feedback with an exponent less than unity, not only unconditionally stabilizes the stall inception point and the neighboring nonaxisymmetric branch, but also it reshapes this branch so as to locally mimic the stable nonaxisymmetric branch at the stall inception point. These results extend and in some places contrast and clarify previous work on this subject that has completely dismissed such linear or sublinear feedback as a useful means of controlling compressor rotating stall.

Appendix A: Evaluation of the MG³ Integrals Using Contour Integration

Consider the two integrals appearing in Eqs. (6) and (7). The integration limits here suggest contour integration in the complex plane along the unit cycle. Use a complex variable z, and define the transformation

$$z = e^{i\theta}, \qquad \mathrm{d}\theta = \frac{\mathrm{d}z}{iz}, \qquad \sin\theta = \frac{z - z^{-1}}{2i} \tag{A1}$$

where i is the imaginary unit. Then, the two integrals can be written as

$$F(\Phi, A) = \frac{1}{2\pi i}\oint_{\text{unit circle}} \Psi\left(\Phi + A\frac{z - z^{-1}}{2i}\right)\frac{\mathrm{d}z}{z} \tag{A2}$$

$$G(\Phi, A) = \frac{1}{2\pi i}\oint_{\text{unit circle}} \Psi\left(\Phi + A\frac{z - z^{-1}}{2i}\right)\left(\frac{z - z^{-1}}{2i}\right)\frac{\mathrm{d}z}{z} \tag{A3}$$

Define two functions $f(z)$ and $g(z)$ by

$$f(z) = \Psi\left(\Phi + A\frac{z - z^{-1}}{2i}\right) \tag{A4}$$

$$g(z) = \Psi\left(\Phi + A\frac{z - z^{-1}}{2i}\right)\left(\frac{z - z^{-1}}{2i}\right) \tag{A5}$$

If Ψ is free of singularities, the only singular point of $f(z)/z$ or $g(z)/z$ within the unit circle is $z = 0$. Then F and G are the residues[12] of $f(z)/z$ and $g(z)/z$ at $z = 0$, respectively. The residue[12] of a function $H(z)$ at a singular point $z = z_s$ is the coefficient of the term $1/(z - z_s)$ in the Laurent series expansion of that function about $z = z_s$. By uniqueness,[12] the Laurent series of $H(z)/z$ about $z = 0$ is the Laurent series of $H(z)$ about $z = 0$, multiplied by $1/z$. Thus, the residues of $f(z)/z$ and $g(z)/z$ at $z = 0$ are the constant terms in the Laurent series of $f(z)$ and $g(z)$ about $z = 0$, respectively. To evaluate these residues, write the ordinary Taylor series of $\Psi(\phi)$ about $\phi = \Phi$. Using this series evaluate Ψ at $\phi = \Phi + A\sin\theta$ and substitute for $\sin\theta$ from Eq. (A1). Then, the functions $f(z)$ and $g(z)$ can be written as

$$f(z) = \sum_{n=0}^{\infty} \frac{\Psi^n(\Phi)(z - z^{-1})^n A^n}{(2i)^n n!} \tag{A6}$$

$$g(z) = \sum_{n=0}^{\infty} \frac{\Psi^n(\Phi)(z - z^{-1})^{n+1} A^n}{(2i)^{n+1} n!} \tag{A7}$$

Superscripts denote differentiation for Ψ and raise to power elsewhere. Recall the binomial formula[17]

$$(x - y)^n = \sum_{\kappa=0}^{n} (-1)^\kappa \binom{n}{\kappa} x^{n-\kappa} y^\kappa \tag{A8}$$

and expand the terms in the parenthesis (for each n) as

$$(z - z^{-1})^n = \sum_{\kappa=0}^{n} (-1)^\kappa \binom{n}{\kappa} z^{n-2\kappa} \tag{A9}$$

$$(z - z^{-1})^{n+1} = \sum_{\kappa=0}^{n+1} (-1)^\kappa \binom{n+1}{\kappa} z^{n+1-2\kappa} \tag{A10}$$

Substituting from Eqs. (A9) and (A10) into Eqs. (A6) and (A7) and summing the coefficients of similar powers in z, we obtain two series, for $f(z)$ and $g(z)$, for which the (integer) powers of z vary from $-\infty$ to $+\infty$. By uniqueness, these are the Laurent series of $f(z)$ and $g(z)$ about $z = 0$. From Eq. (A9), a constant term is contributed to the Laurent series for $f(z)$ each time n is even. This is the term for which $n = 2\kappa$. It is equal to

$$\frac{\Psi^{2\kappa}(\Phi)(-1)^\kappa A^{2\kappa}}{(2i)^{2\kappa}(2\kappa)!}\binom{2\kappa}{\kappa}$$

The sum of all such terms for $\kappa = 0, 1, 2, \ldots$, is the residue of $f(z)/z$ about $z = 0$ that in turn equals F. With[17]

$$\binom{2\kappa}{\kappa} = \frac{(2\kappa)!}{\kappa!(2\kappa - \kappa)!} = \frac{(2\kappa)!}{(\kappa!)^2} \tag{A11}$$

this leads to $F(\Phi, A)$ supplied in Eq. (11). Similarly, from Eq. (A10), a constant term is contributed to the Laurent series for $g(z)$ about $z = 0$ each time $n + 1$ is even. This is the term for which $n + 1 = 2\kappa$, and it is equal to

$$\frac{\Psi^{2\kappa-1}(\Phi)(-1)^\kappa A^{2\kappa-1}}{(2i)^{2\kappa}(2\kappa - 1)!}\binom{2\kappa}{\kappa}$$

The sum of all such terms for $\kappa = 1, 2, 3, \ldots$, is the residue of $g(z)/z$ about $z = 0$, which in turn equals G. Through Eq. (A11) this leads to $G(\Phi, A)$ supplied in Eq. (12). The series representation of these integrals is valid as long as certain obvious smoothness properties on $\Psi(\phi)$ are satisfied.

Appendix B: Generating Function for the MG³ Integrals

The two MG integrals [Eqs. (11) and (12)] can be generated from a single function by partial differentiation. Let

$$Q(\Phi, A) = \sum_{\kappa=0}^{\infty} \frac{\Psi^{2\kappa-1}(\Phi)}{(\kappa!)^2}\left(\frac{A}{2}\right)^{2\kappa} \tag{B1}$$

where for $\kappa = 0$, characteristic $\Psi^{-1}(\Phi)$ denotes the indefinite integral of $\Psi(\Phi)$. Then it is easy to show that F and G are

$$F(\Phi, A) = \frac{\partial Q}{\partial \Phi}, \qquad G(\Phi, A) = \frac{\partial Q}{\partial A} \tag{B2}$$

The partial derivatives of F and G with respect to Φ and A are, thus, given by

$$\frac{\partial F}{\partial \Phi} = \frac{\partial^2 Q}{\partial \Phi^2} = \sum_{\kappa=0}^{\infty} \frac{\Psi^{2\kappa+1}(\Phi)}{(\kappa!)^2}\left(\frac{A}{2}\right)^{2\kappa} \tag{B3}$$

$$\frac{\partial G}{\partial A} = \frac{\partial^2 Q}{\partial A^2} = \sum_{\kappa=1}^{\infty} \frac{\kappa(2\kappa - 1)\Psi^{2\kappa-1}(\Phi)}{2(\kappa!)^2}\left(\frac{A}{2}\right)^{2\kappa-2} \tag{B4}$$

$$\frac{\partial F}{\partial A} = \frac{\partial G}{\partial \Phi} = \frac{\partial^2 Q}{\partial \Phi \partial A} = \sum_{\kappa=1}^{\infty} \frac{\kappa\Psi^{2\kappa}(\Phi)}{(\kappa!)^2}\left(\frac{A}{2}\right)^{2\kappa-1} \tag{B5}$$

Acknowledgment

This work was supported by the U.S. Army Research Office, Grant DAAH04-96-1-0008 for the Multidisciplinary University Research Initiative (MURI) on Intelligent Turbine Engines, David Mann, Grant Monitor.

References

[1] Krstic, M., Protz, J. M., Paduano, J. D., and Kokotovic, P. V., "Backstepping Designs for Jet Engine Stall and Surge Control," Proceedings of the 34th Conf. on Decision and Control, New Orleans, LA, Vol. 3, Dec. 1995, pp. 3049–3055.

[2] Eveker, K. M., Gysling, D. L., Nett, C. N., and Sharma, O. P., "Integrated Control of Rotating Stall and Surge in Aeroengines," Proceedings of the SPIE Conf. on Sensing, Actuation and Control in Aeropropulsion, Vol. 2494, April 1995, pp. 21–35.

[3] Moore, F. K., and Greitzer, E. M., "A Theory of Post-Stall Transients in Axial Compressor Systems, Part I, Development of Equations," *Journal of Turbomachinery*, Vol. 108, Jan. 1986, pp. 68–76.

[4] Moore, F. K., and Greitzer, E. M., "A Theory of Post-Stall Transients in

Axial Compressor Systems, Part II, Application," *Journal of Turbomachinery*, Vol. 108, April 1986, pp. 231–239.

[5]Badmus, O. O., Chowdhury, S., Eveker, K. M., Nett, C. N., and Rivera, C. J., "Simplified Approach for Control of Rotating Stall, Part 1: Theoretical Development," *Journal of Propulsion and Power*, Vol. 11, No. 6, Nov.–Dec. 1995, pp. 1195–1209.

[6]Badmus, O. O., Chowdhury, S., Eveker, K. M., Nett, C. N., and Rivera, C. J., "Simplified Approach for Control of Rotating Stall, Part 2: Experimental Results," *Journal of Propulsion and power*, Vol. 11, No. 6, Nov.–Dec. 1995, pp. 1210–1223.

[7]Liaw, D.-C., and Abed, E. H., "Stability Analysis and Control of Rotating Stall," *IFAC Symposia Series*, No. 3, 1993, pp. 295–300.

[8]Badmus, O. O., "Nonlinear Dynamic Analysis and Control of Surge and Rotating Stall in Axial Compression System Models," Ph.D. Thesis, Georgia Inst. of Technology, Atlanta, GA, 1994, pp. 64–80, 139–152.

[9]Chowdhury, S., "An Experimental Investigation of Active Stall Control in Compression Systems," Ph.D. Thesis, Georgia Inst. of Technology, Atlanta, GA, 1995, pp. 87–92.

[10]Abed, E. H., and Hu, J.-H., "Local Feedback Stabilization and Bifurcation Control, I. Hopf Bifurcation," *Systems and Control Letters*, Vol. 7, 1986, pp. 11–17.

[11]Abed, E. H., and Hu, J.-H., "Local Feedback Stabilization and Bifurcation Control, II. Stationary Bifurcation," *Systems and Control Letters*, Vol. 8, 1987, pp. 467–473.

[12]Churchill, R. V., and Brown, J. W., *Complex Variables and Applications*, McGraw–Hill, New York, 1984, pp. 132–165.

[13]Verhulst, F., *Nonlinear Differential Equations and Dynamical Systems*, Springer–Verlag, Berlin, 1990, pp. 101–114, 193–197.

[14]Perko, L., *Differential Equations and Dynamical Systems*, 2nd ed., Springer–Verlag, Berlin, 1996, pp. 129–161.

[15]Guckenheimer, J., and Holmes, P., *Nonlinear Oscillations, Dynamical Systems, and Bifurcations of Vector Fields*, 2nd printing, Springer–Verlag, Berlin, 1986, pp. 123–138.

[16]DiStefano, J. J., Stubberud, A. R., and Williams, I. J., *Feedback and Control Systems*, 2nd ed., Schaum's Outline Series, McGraw–Hill, New York, 1990, pp. 115, 116.

[17]Spiegel, M. R., *Mathematical Handbook of Formulas and Tables*, Schaum's Outline Series, McGraw–Hill, New York, 1968, pp. 3, 4.